



The growth of photorefractive planar BTO/BSO and BTO/BGO waveguide

Yu.F. Kargin^{a,*}, A.V. Egorysheva^a, V.V. Volkov^a, M.N. Frolova^b,
M.V. Borodin^b, S.M. Shandarov^b, V.M. Shandarov^b, Detlef Kip^c

^a*Kurnakov Institute of General and Inorganic Chemistry of Russian Academy of Sciences, Leninsky prospect 31, 119991 Moscow, Russian Federation*

^b*State University of Control Systems and Radioelectronics, 40 Lenin Avenue, Tomsk 634050, Russian Federation*

^c*Technical University of Clausthal, Physics Institute, Leibnitzstr.4, 38678 Clausthal-Zellerfeld, Germany*

Available online 7 January 2005

Abstract

The $\text{Bi}_{12}\text{TiO}_{20}$ thin films with high optical quality were grown from the melt on a substrate of $\text{Bi}_{12}\text{SiO}_{20}$ and $\text{Bi}_{12}\text{GeO}_{20}$ single crystals by two methods: LPE and crystallization from finite volume (CFV). The results of experimental investigation of time evolution of light-induced absorption in BTO:Cu waveguide are presented. All structures show a nearly equidistant spectrum of n_{eff} with intervals from 2×10^{-3} to 5×10^{-3} . The time evolution of light-induced absorption is qualitatively different for the lowest and the highest modes in the waveguide.

© 2004 Elsevier B.V. All rights reserved.

PACS: 78.20.E; 72.40+W; 78.90+t

Keywords: A2. Top-seeded solution growth; B1. Bismuth compounds; B1. Oxides; B2. Photorefractive materials

1. Introduction

The interaction of light waves in photorefractive crystals plays an important role in development of devices for optical data processing. $\text{Bi}_{12}\text{M}_x\text{O}_{20\pm\delta}$ (M—elements of II–VIII groups or their combina-

tions) crystals with sillenite-type structure are advanced materials for integrated optics. $\text{Bi}_{12}\text{TiO}_{20}$ (BTO) is a photorefractive crystal, which has numerous applications in two-beam coupling, and four-wave mixing experiments. The light propagation through photorefractive waveguide can give rise to extend the light band intensity, which is important for development of integrated optic modulator [1–4].

The effects of photoinduced absorption of light [4,5] and two-beam interactions on photorefractive

*Corresponding author. Tel.: +7959554802;

fax: +7959541279.

E-mail address: Yu.kargin@rambler.ru (Y.F. Kargin).

grating [6,7] in planar waveguides based on sillenites were observed.

In the present work, results of research of characteristics of the planar optical waveguides of BTO deposited on $\text{Bi}_{12}\text{SiO}_{20}$ (BSO) and $\text{Bi}_{12}\text{GeO}_{20}$ (BGO) substrates are presented.

2. Technology of formation of waveguides

The BTO thin films with high optical quality were grown on a substrate of BSO and BGO single crystals by crystallization from the melt. The substrate wafers, representing the plates with the cross sizes $20 \times 30 \text{ mm}^2$ and thickness of 2–4 mm, have been preliminarily cut from the boules along the $\langle 110 \rangle$ or $\langle 100 \rangle$ axes and subsequently polished flat and parallel. The following epitaxial layers both of undoped and doped BTO have been deposited on BGO (BSO) substrates by LPE method or crystallization from finite volume (CFV): BTO/BSO, BTO/BGO, BTO<Cu>/BSO, BTO<Cu>/BGO, BTO<Ca + Ga>/BGO. The initial composition of the melt has the concentration of 7.0 or 8.0 mol% TiO_2 . Doping of the crystals with Cu, Ca, and Ga is performed by adding the corresponding oxides in amount of 0.1 wt% to the melt. In a typical LPE experiment, the substrate is dipped into a Pt crucible ($\sim 50 \text{ cm}^3$) with a slightly supercooled melt of the desired film composition. The actual degree of supercooling of the melt produces growth rate in order of 1–2 $\mu\text{m}/\text{min}$. Growth of epitaxial layers was carried out at constant supercooling of the melt at 2–4 °C relative to the liquidus curve. The crystals were grown over a period of time, which allowed the production of layers from 50 up to 150 μm . These heterostructures were pulled out from the melt and cooled at a rate no more than 40 °C h^{-1} . In CFV the uniform layer of BTO dispersed powder, whose amount provided crystallization of a layer with thickness 200–300 μm , was placed onto (100)- or (110)-oriented BSO (or BGO) wafers. Thereafter this structure was placed in a platinum cuvette and put into a resistance furnace. The furnace was heated at a rate of $\sim 60^\circ \text{ h}^{-1}$ to the melting point of BTO. After the formation of the layer of BTO melt, the furnace was cooled at a rate of 0.1 °C h^{-1} to the

temperature of 800 °C. 15 min of heating at melting point allows to grow high-quality bubble-free BTO thin films. Then the cooling rate was increased to 30–60 °C h^{-1} . An as-grown layer was subsequently polished up to 15–50 μm thickness.

He–Ne laser with wavelength of $\lambda = 0.633 \text{ nm}$ and capacity of radiation $P_0 = 40 \text{ mW}$ was used in experiments with waveguide characteristics and absorption photoinduced effects. We have used rutile or GaP prisms to coupler beams of He–Ne laser into and out of the waveguide. Measurement of a spectrum mode of optical waveguides was carried out by a standard technique [8].

3. Waveguide properties of epitaxial structures

The basic characteristics of the waveguide 1 received by a method of CFV, and the waveguides 2–10, which have been prepared by crystallization from a solution in the melt, are shown in Table 1.

The effective refractive indices n_{eff} of the TE and TM modes for fabricated sillenite structures were measured by the method of prism coupling at the light wavelength of 633 nm. All structures show practically an equidistant spectrum of n_{eff} with intervals from 2×10^{-3} to 5×10^{-3} suggesting that the profile of refractive index for a waveguide layer can be approximated by the parabolic function:

$$n(x) = n_w - \Delta n \frac{x^2}{h_w^2}, \quad (1)$$

where n_w is the refractive index of waveguide layer at the interface with a cover, and Δn and h_w are the parameters of parabolic distribution. The parameters n_w , Δn , and h_w as well as a number of the feasible TE modes for some fabricated structure are presented in Table 1. We also observed in the studied waveguides the TM modes with the same intervals in a spectrum of n_{eff} as for TE modes.

4. Light-induced absorption in waveguide structure BTO:Cu/BSO

Time evolution of light-induced absorption is studied for the waveguide involving BTO:Cu layer

Table 1
Examples of fabricated planar waveguides

Waveguide layer	Substrate and its orientation	Refractive index n_w	Parameters of parabolic profile		Number of TE modes
			Δn	h_w (μm)	
1. BTO	BGO (1 1 0)	2.557	0.0004 for lower modes	30	40
2. BTO	BGO (1 1 0)	2.556	0.019	12	9
3. BTO:Cu, 0.11 wt% Cu	BSO (1 0 0)	2.535	0.030	15	7
4. BTO	BSO (1 1 0)	2.586	0.050	10	10
5. BTO, 8 mol% TiO_2 in a mixture	BGO (1 1 0)	2.552	0.027	10	9
6. BTO	BSO (1 1 0)	2.550	0.012	4	3
7. BTO	BSO (1 0 0)	2.561	0.020	13	9
8. BTO, 7 mol% TiO_2 in a mixture	BSO (1 1 0)	2.577	0.024	8	7
9. BTO:Cu, 0.11 wt% Cu	BSO (1 1 0)	2.555	0.030	20	15
10. BTO:Ca + Ga	BSO (1 1 0)	2.560	0.026	20	14

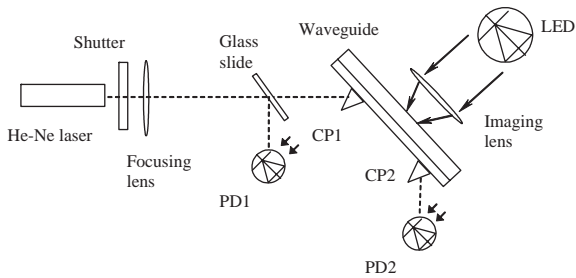


Fig. 1. The experimental setup for the investigation of light-induced absorption in planar waveguides.

formed on the (1 0 0)-cut BSO substrate (see row 3 in Table 1). The scheme of the experimental setup is shown in Fig. 1. The light beam emerging from a He–Ne laser with wavelength of 633 nm is turned on and off by a shutter to observe the build up and dark decay of light-induced absorption. The beam is focused and coupled to the waveguide by the coupling prism CP1. The input light is also split by glass slide GS and monitored by photodiode PD1. The output light is in-coupled from the waveguide by prism CP2 and its power is measured by photodiode PD2. Between the experiments, the waveguide was screened from extraneous illumination by an opaque box. During the experiments, the waveguide can be illuminated through the substrate by an incoherent red (wavelength of 660 nm) or green (525 nm) radiation from the light-

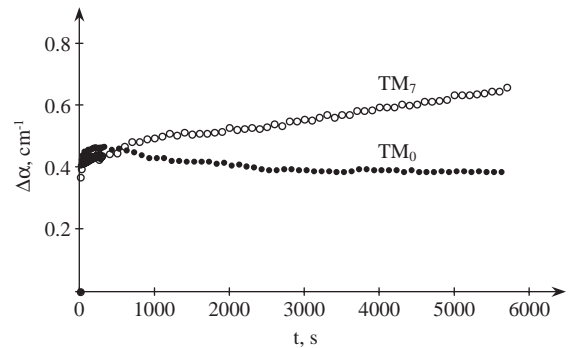


Fig. 2. Evolution of the changes in the absorption coefficient $\Delta\alpha(t)$ for TM_0 and TM_7 modes in the waveguide BTO:Cu/BSO.

emitting diode (LED). The imaging lens allows for illumination of the waveguide layer between coupling prisms by ring spot with a diameter of 3 mm and with maximal intensity of 50 and 8 mW/cm^2 for red and green light, respectively.

The time dependences of changes in light absorption, $\Delta\alpha(t)$, self-induced on the modes TM_0 and TM_7 in the waveguide are shown in Fig. 2. One can see that the time evolution of light-induced absorption is qualitatively different for the lowest and the highest modes. In particular, dependence $\Delta\alpha(t)$ has a non-monotonous behavior for TM_0 mode. A slow prolonged component of light-induced absorption is observed both for TM_0 and TM_7 modes. However, this component causes

the decrease in light absorption for TM_0 mode and growth for TM_7 mode at $t > 200$ s. It is assumed [9,10] that the defect donor and trap centers are responsible for light-induced absorption in sillenite crystals. The observed distinctions indicate that these centers have an inhomogeneous distribution on the depth of epitaxial structure BTO:Cu/BSO.

Fig. 3 shows typical time dependence for build up and dark decay of light-induced absorption for TM_0 mode. Upon turning on the laser beam at $t > 0$ time behavior of $\Delta\alpha(t)$ is the same as in Fig. 2. Turning off of this beam at $t = 2100$ s results in the decay of induced changes in the waveguide. Thereafter the beam is turned on during the short interval ~ 3 s only to measure the changes in $\Delta\alpha(t)$. It can be seen that the exciting TM_0 mode in this case causes the growth in light absorption of no more than 0.03 cm^{-1} . The dark decay during 3300 s results in waveguide light absorption approximately the same as before the start of this experiment. However, the behavior of $\Delta\alpha(t)$ after the second turning on the beam at $t = 5400$ s for a long time does not replicate one at $0 < t < 2100$ s. This suggests that illumination of the waveguide layer by TM_0 mode causes a redistribution of charge carriers on the donor and trap defect centers. However, the resulting distributions for the charged and neutral defects have a complicated pattern and do not decay to an initial form during the time used for dark exposure.

We did not observe the noticeable changes in absorption for all waveguide TM modes under the illumination of the epitaxial structure by red

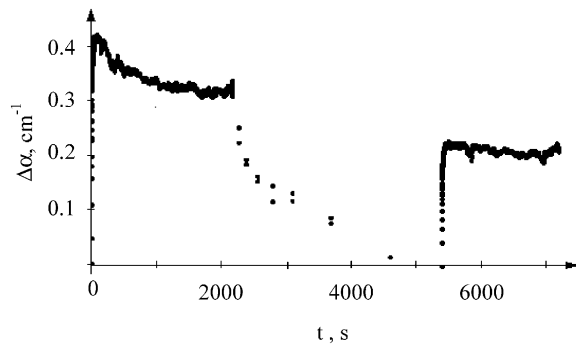


Fig. 3. Build up and dark decay of light-induced absorption for TM_0 mode in the waveguide BTO:Cu/BSO.

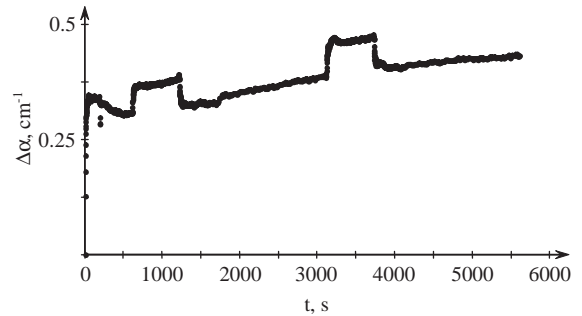


Fig. 4. Evolution of light-induced absorption at TM_0 mode in the structure BTO:Cu/BSO at the additional illumination of waveguide layer by green incoherent light during the time intervals from 600 to 1200 s and from 3000 to 3600 s.

incoherent light (see Fig. 1) with the wavelength of 660 nm and intensity of 50 mW/cm^2 . The illumination of the waveguide by green light (525 nm, 8 mW/cm^2) from LED turned on at $t = 600$ and 3000 s results in the increasing of TM_0 -mode absorption (633 nm) approximately at 0.08 cm^{-1} (Fig. 4). A comparison of Figs. 3 and 4 shows that green illumination of the waveguide causes qualitative modification of a time evolution of light-induced absorption for TM_0 mode at a wavelength of 633 nm: instead of the decrease for $\Delta\alpha(t)$, its growth at $t > 1200$ s is observed. We also observed in the experiments the decrease in a sensitivity of waveguide absorption to green illumination with the number of TM modes. This kind of behavior confirms the assumption relative to an inhomogeneity in distributions of the donor and trap centers on the waveguide layer because the depth where the main power of waveguide mode is transferred increases with its number.

5. Conclusion

The characteristics of the planar optical waveguides BTO/BGO, BTO:Cu/BSO at various orientations are investigated. The dynamics of the absorption coefficient variation in a planar photo-refractive BTO/BSO waveguide has been studied. It has been shown that their optical absorption may significantly change due to irradiation by low-intensity incoherent green light from LEDs. This fact suggests that the optical control of

photorefractive soliton characteristics in such waveguides is possible.

Acknowledgment

This work was supported by INTAS under the Project 01-0481.

References

- [1] P. Gunter, J.P. Huignard (Eds.), *Photorefractive Materials and Their applications I*, Topics in Applied Physics, vol.61, Springer, Berlin, 1988.
- [2] P.V. Petrov, S.I. Stepanov, A.V. Khomenko, *Fotorefraktivnye Kristally v Kogerentnoi Optike (Photorefractive Crystals in Cogerent Optics)*, Nauka, St. Petersburg, 1992.
- [3] M.N. Frolova, M.V. Borodin, S.M. Shandarov, V.M. Shandarov, Yu.F. Kargin, A.V. Egorysheva, D. Kip, *Trends Opt. Photonics* 87 (2003) 403.
- [4] V.I. Burkov, A.V. Egorysheva, Yu.F. Kargin, *Russ. Crystallogr. Rep.* 46 (2001) 356 (Engl. trans).
- [5] S.Yu. Veretennikov, A.T. Mandel, S.M. Shandarov, M.I. Tzurkan, A.V. Kazarin, A.M. Plesovskih, A.V. Egorysheva, Yu.F. Kargin, O.N. Bikeev, V.V. Shepelevich, *Izv. Vuzov. Fiz.* (2) (2003) 39 (in Russian).
- [6] E.I. Leonov, S.E. Habarov, A.A. Lipovskii, V.M. Abusev, *Zh. Tekh. Fiz.* 58 (1988) 2181 (in Russian).
- [7] Yu.F. Kargin, Yu.R. Salikaev, S.M. Shandarov, I.V. Tzisar, *Pisma v Zh. Tekh. Fiz.* 20 (1994) 55 (in Russian).
- [8] Yu.R. Salikaev, S.M. Shandarov, Yu.F. Kargin, *Proc. SPIE* 2795 (1996) 203.
- [9] M.N. Frolova, M.V. Borodin, S.M. Shandarov, V.M. Shandarov, Y.F. Kargin, A.V. Egorysheva, D. Kip, *Europhysics Conference Abstracts* vol. 27E CF3-6-TUE, 2003.
- [10] A.E. Mandel, A.M. Plesovskih, S.M. Shandarov, M.I. Tzurkan, K.S. Plinta, Yu.F. Kargin, V.V. Volkov, A.V. Egorysheva, V.V. Shepelevich, V.N. Navyko, *Izv. Vuzov. Fiz.* (12) (2003) 48 (in Russian).